

Engineered Pigment Nanoparticles: Bottom-up Synthesis, Characterization, and Performance Properties

Rina Carlini,* Darren A. Makeiff,** C. Geoffrey Allen,* Sandra J. Gardner,*
Francisco Paraguay-Delgado,** Marek Malac,** Peng Li**

*Xerox Research Centre Canada, Mississauga, ON, Canada ; rina.carlini@xerox.com

**National Institute for Nanotechnology, Edmonton, AB, Canada ; darren.makeiff@nrc.gc.ca

ABSTRACT

High performance organic nanopigments are an increasingly important class of functional nanomaterials that possess physical properties ranging between molecular and bulk materials. These nanomaterials have been utilized in a variety of important commercial applications including coatings, printing, information storage, and display technologies [1]. We will discuss our recent work in developing a bottom-up approach for preparation of 3 different classes of high-performance organic nanopigments: 1) azo-laked Pigment Red 57:1 (LAK), 2) quinacridone Pigment Red 122 (QUIN), and 3) azo-benzimidazolone (BZI) Pigments Yellow 151 and Red 175. The physical characteristics of the nanopigments were characterized by electron microscopy, dynamic light scattering (DLS), and powder X-ray diffraction (XRD), while their coloristic spectral properties, and dispersion thermal stability were investigated in various matrices. We identified relationships between pigment particle size and their coloristic as well as thermal stability properties for these nanopigments. High resolution transmission electron microscopy (HR-TEM) provided clear images of lattice fringes, and enabled us to determine the crystal orientation of the molecules packed within the QUIN and BZI pigment nanoparticles.

Keywords: nanoparticles, nanopigment, organic pigment, electron microscopy, X-ray diffraction.

INTRODUCTION

We have developed a general bottom-up synthesis approach to designing nanopigments that involve controlled assembly of building block molecules and/or pigment precursors. A key objective was to prepare the pigment nanoparticles with low aspect ratio (LxW) and also with unique surface chemistry that would ensure optimum thermal stability and dispersion performance, without altering the inherent pigment physical properties (crystal structure, thermal properties). Depicted in Figure 1, our approach involved steric stabilization and the use of pigment-affinic amphiphiles that both target and regulate the self-assembly of colorant molecules into pigment nanoparticles. This versatile design was applied to three

structurally different classes of high performance pigments that are used in coating and printing applications, including azo-laked PR 57:1, quinacridone pigment PR 122, and benzimidazolone pigments PY 151 and PR 175.

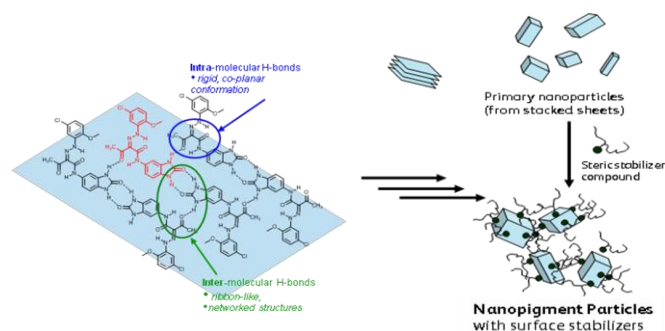


Figure 1: General approach for bottom-up assembly of organic nanopigments.

High performance pigments are so-called because they have excellent thermal and photostability and superior solvent fastness, which is the result of inter and intramolecular hydrogen (H) bonding present in the crystalline state (Fig. 2 for PY 151) [2]. Most commercial organic pigments are anisotropic particles having large LxW aspect ratios of greater than 5:1, which is often a consequence of the extensive H-bonding networks. We have obtained detailed characterization of the example BZI, QUIN and LAK pigment nanoparticles, by various electron microscopies, powder X-ray diffraction spectroscopy, CIELAB color properties, thermal stability in liquid solvent dispersions and lightfastness in dispersed polymer films.

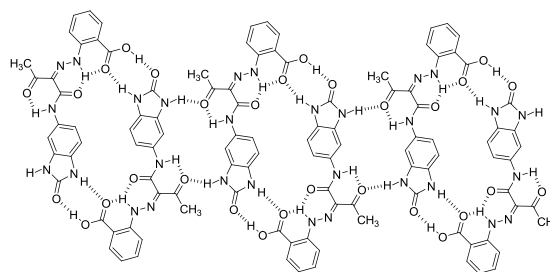


Figure 2. Hydrogen-bonded chains of PY151 molecules from the reported crystal structure [2].

RESULTS AND DISCUSSION

Both the LAK and BZI pigment nanoparticles were synthesized using standard diazotization-coupling reactions from appropriate starting materials, while the QUIN nanopigments were prepared by either direct synthesis or by reprecipitation of bulk commercial pigment [3, 4]. The dimensions and 3D morphologies of BZI (PY 151) and QUIN (PR 122) nanopigments were determined by DLS, SEM, HR-TEM and energy-filtered TEM (EF-TEM) methods. The imaging revealed elongated brick-shaped nanoparticles for PY 151 (Fig. 3a) with average dimensions of $L=80$ nm, $W = 25$ nm and average thickness of $T = 24$ nm, while for PR 122, the nanoparticles had dimensions of $L = 73 \pm 32$ nm and $W = T = 19 \pm 8$ nm. Both of these nanopigment examples had ($L \times W$) aspect ratio ≈ 2 -3, which represents a 2 to 3-fold reduction compared with commercial version of these pigments.

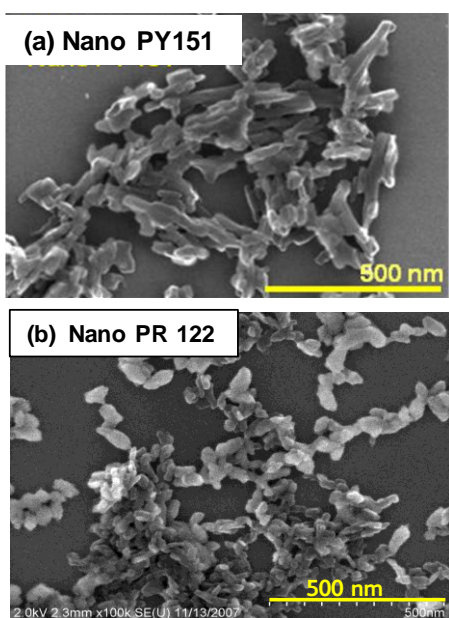
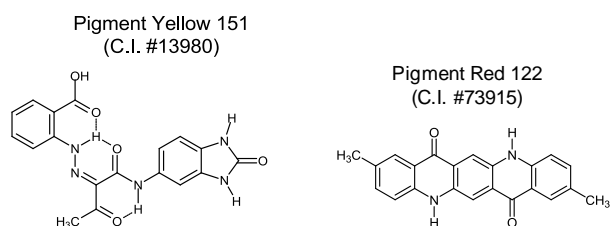


Figure 3. SEM image of (a) PY151 nanoparticles, and (b) PR 122 pigment nanoparticles

We obtained powder XRD and HR-TEM imaging data for both PR 122 and PY 151 nanopigments, in order to elucidate molecular packing within these nanoparticles. The molecular packing within the PY 151 nanoparticles is the same polymorph as in the recently reported crystal structure for PY151 [2], which suggests that the pigment-affinic

amphiphilic additives introduced during synthesis must not significantly disrupt the crystal packing in order to reduce particle size, but rather associate weakly on the pigment particle surfaces. Fig. 4 shows an HR-TEM image of PY151 nanoparticles, whereby distinct lattice planes were observable with a d -spacing of 1.6 nm, likely corresponding to the (001) planes based on the reported PY 151 crystal structure [4]. The observed lattice planes enabled us to determine the orientation of the hydrogen-bonded chains of PY151 molecules.

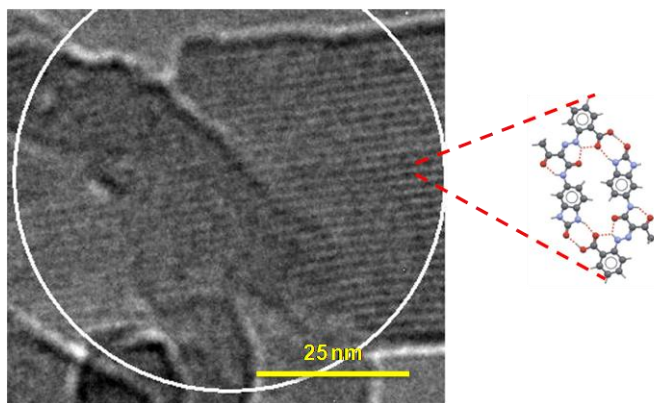


Figure 4. HR-TEM image of PY 151 nanoparticles.

CONCLUSIONS

A general design and method for bottom-up assembly of pigment nanoparticles was developed for three classes of high performance organic pigments. A detailed understanding of pigment nanoparticles structure is important in order to develop these nanomaterials with tunable performance properties.

REFERENCES

- [1] Herbst, W.; Hunger, K. *Industrial Organic Pigments: Production, Properties, Applications*; Wiley-VCH: Weinheim, Germany, 2004.
- [2] van der Streek, J.; Ivashevskaya, S. N.; Ermrich, M.; Paulus, E. F.; Bolte, M.; Schmidt, M. U. *Acta Cryst.* **2009**, B65, 200-211.
- [3] a) US Patent Application No. 20100004360A1, Xerox Corporation and National Research Council of Canada. b) US Patent Application No. 20100037955A1; Xerox Corporation and National Research Council of Canada. c) *US Patent No. 7,503,973*; 03/17/2009, Xerox Corporation.
- [4] a) Xerox Corporation, US Patent No. 7,427,323; 2008; b) Xerox Corporation, US Patent No. 7,534,294; c) Xerox Corporation, US Patent No. US 7,465,348; 7,473,310.